2021 43rd Annual International Conference of the
IEEE Engineering in Medicine & Biology Society (EMBC)
Oct 31 - Nov 4, 2021. Virtual Conference

Inverse Kinematics of a Parallel Mechanism with an Offset Structural Design for Prosthetic Wrist Motions

Hojin Seo, Amshumanth Chakragiri, Maanas Purushothapu, Seungcheol Lee, and Woon-Hong Yeo*

***Abstract*— Recent developments in upper limb wrist prosthetics allow for amputees to closely mimic the motions of a healthy human wrist. Although many active wrist prosthetics can flex and extend, relatively little work is done with their ability to pronate and supinate without the use of additional motors between the region where the forearm meets the hand. This paper reports a 3SPS-S-3RRR mechanism that provides quasi-spherical motions, mimicking a wrist's ability to flex and extend. It is also designed to offer rotational motion with offset Kresling arms to achieve motions conforming with pronation and supination. The paper explores the kinematics of the mechanism and introduces the use of motion capture acquisition in further studies.**

I. Introduction

There are approximately 50,000 new major limb amputations every year in the United States, and prosthetic devices offer a way for the amputees to mimic the motions of a healthy human upper limb. [1] [2] Compact, lightweight, and active prosthetic wrists are needed for the comfort of trans-radial amputees, but many prosthetic wrist devices are lightweight and compact at the expense of complexity in motion. On the other hand, many prosthetic wrist devices that can provide the motion range of pronation and supination make use of additional motors, which in turn, increases the overall weight of the device. [3] [4] [5]

Parallel mechanisms have been recently introduced to provide an alternative to conventional prosthetic wrist devices. The apparent advantages include but are not limited to its weight, quasi-spherical motions, and its compatibility with tendon-actuated designs. The disadvantages include its size, the lack of pronating and supinating motions, and difficulty in controls. [6] [7] [8] Limited prior works have been done to design a quasi-spherical parallel mechanism for wrist prosthetics that are able to pronate and supinate. [9] [10] This paper makes use of a Kresling arm resembling the Kresling patterns in origami to allow pronating and supinating motions for a spherical parallel manipulator.

II. Mechanism Descriptions

The human wrist presents a set of complex motions with a combination of extension/flexion, pronation/supination, and radial/ulnar deviation, as shown in fig. 1(a). [11] It is also commonly modelled as a saddle joint or a condyloid joint, as illustrated in fig. 1(b). Most prosthetic devices are modelled to provide the motion range of a saddle joint or a condyloid joint, but the proposed design aim to provide a rotational motion in addition to the conventional 2-DOF motion. [12]

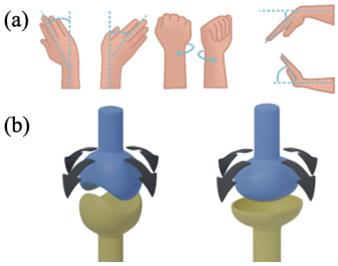

Figure 1. Illustration of basic human wrist motions including flexion/extension, ulnar/radial deviation, and pronation/supination (a). Saddle joint and condyloid joint (b).

As a starting point, a conventional 3SPS mechanism was proposed to offer spherical motion. Three prismatic kinematic chains are attached to the base circular plate, and are expected to provide the full range of quasi-spherical flexion/extension motion. A prismatic chain is attached to the center for simplicity in controls.

An offset structural 3RRR design is introduced to account for the rotational motions. These kinematic arms are inspired by Kresling folds in origami. Kresling origami originates from the buckling and collapsing deformation of a cylindrical shell under compression. [13] These structures, with the prismatic chains, are expected to provide a spinning motion to the upper circular plate from its height differences. Fig. 2(a) and 2(b) shows the assembly of the mechanism.

H. Seo is with the George W. Woodruff School of Mechanical Engineering, College of Engineering, Georgia Institute of Technology, Atlanta, GA 30332 USA (e-mail: hseo47@gatech.edu).

A. Chakragiri is with the Wallace H. Coulter Department of Biomedical Engineering, College of Engineering, Georgia Institute of Technology, Atlanta, GA 30332 USA (e-mail: achakragiri@gatech.edu).

M. Purushothapu is with the School of Electrical and Computer Engineering, College of Engineering, Georgia Institute of Technology, Atlanta, GA 30332 USA (e-mail: mpurushothapu8@gatech.edu).

S. Lee is with the Faculty of Arts and Humanities, Coventry University, CV1 5FB UK (e-mail: lees153@uni.coventry.ac.uk).

*W. H. Yeo is with George W. Woodruff School of Mechanical Engineering, Center for Human-Centric Interfaces and Engineering, Wallace H. Coulter Department of Biomedical Engineering, Parker H. Petit institute for Bioengineering and Biosciences, Georgia Institute of Technology, Atlanta, GA 30332 USA (phone: 404-385-5710; e-mail: whyeo@gatech.edu).

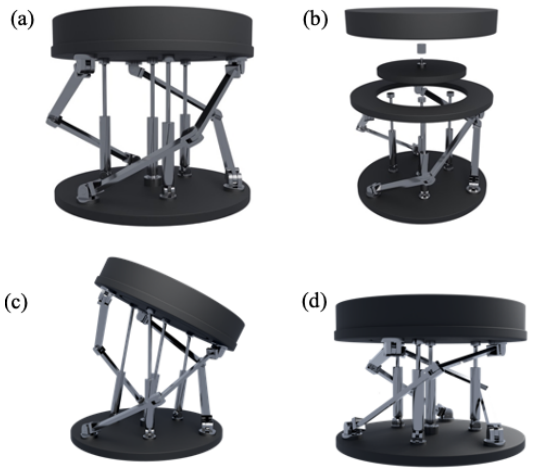

Figure 2. Assembly of the 3SPS-S-3RRR mechanism (a), exploded view of the assembly (b). Assembly of the mechanism while flexing and extending (c), and while pronating and supinating (d).

III. Kinematics of Mechanism

This section first explores the kinematics of the offset 3RRR Kresling arms during a spinning motion as shown in fig. 2(c), then the entire mechanism including flexion and extension as in fig. 2(d) with screw theory.

A. Forward Kinematics of the 3RRR

The Denavit-Hartenburg (D-H) rule is used for the forward kinematics of the Kresling arm to result in a homogeneous transformation matrix. The frames are defined as shown in fig. 3, and the D-H parameters are as presented in table 1.

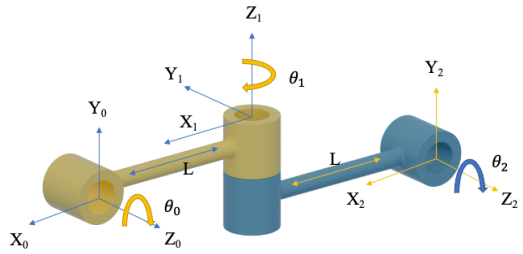

Figure 3. 3RRR frame diagram.

TABLE I. D-H Parameters of the 3 RRR

	D-H Parameters			
	$\boldsymbol{\theta}$	$\boldsymbol{\alpha}$	$\boldsymbol{r}$	$\boldsymbol{d}$
1	$\boldsymbol{\theta_0}$	$-\frac{\pi}{4}$	L	0
2	$\boldsymbol{\theta_1}$	$\frac{\pi}{4}$	L	0

The end-to-end transformation matrix from the D-H parameters is written as:

$$ {}^{0}_{2}T = \begin{bmatrix} c\theta_0 & -s\theta_0 & 0 & -\frac{\pi}{4} \\ 0 & 0 & 1 & 0 \\ s\theta_0 & -c\theta_0 & 0 & 0 \\ 0 & 0 & 0 & 1 \end{bmatrix}. \quad (1) $$

B. Inverse Kinematics of the 3RRR

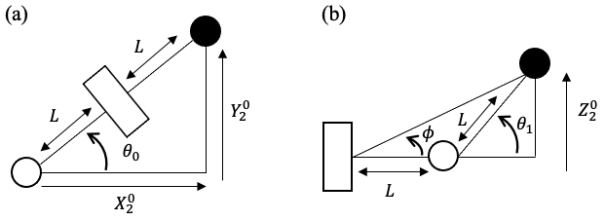

Figure 4. Top-view (a) and side-view (b) of the 3 RRR manipulator.

Fig. 4 shows the top-view and the side-view of the manipulator that indicates the parameters for inverse kinematics. Inverse kinematics of a kinematic chain describes the joint parameters given the end-effector position. [14] The joint parameters θ_0 and θ_1 are the rotational angle along with the Z axis in frame 0 and 1 respectively. ϕ is defined as the angle between the end-to-end joints in sideview. The parameters are defined as:

$$ \theta_1 = tan^{-1}\left(\frac{Y_2^0}{X_2^0}\right) \quad (2) $$

$$ \theta_2 = sin^{-1}\left(\frac{Z_2^0}{L}\right) \quad (3) $$

$$ \theta_1 = tan^{-1}\left(\frac{Z_2^0}{L+\sqrt{L^2++(Z_2^0)^2}}\right). \quad (4) $$

C. Inverse Kinematics of the 3SPS-S-3RRR

The mechanism can be represented as series of linear combination of screws, where the end-effector velocity is denoted as $\{{}^b\omega^t; {}^bv^t\}$. [15] Plücker coordinates and the reference frames are defined in fig. 5.

For each kinematic chain modelled for 3(SPS)-S, the velocity equation is written as

$$ \{{}^b\omega^t; {}^bv^t\} = \{0,0\}_i {}^b\$^1{}_i + \left({}_1v_2\right)_i {}^1\$^2{}_i + \left({}_2\omega_3\right)_i {}^2\$^3{}_i + \left({}_3\omega_4\right)_i {}^3\$^4{}_i + \left({}_4\omega_5\right)_i {}^4\$^5{}_i + \left({}_5\omega_t\right)_i {}^5\$^t{}_i. \quad (5) $$

Since ${}^b\$^1$ is fixed to the lower platform, the velocity is $\{0, 0\}$. ${}_1\omega_2$ is 0 because ${}^1\$^2$ models a prismatic joint. The spherical joints are modelled as three revolute joints ${}^2\$^3$, ${}^3\$^4$, and ${}^4\$^5$.

Similarly, the 3 RRR kinematic chain can be written as

$$ \{{}^b\omega^t; {}^bv^t\} = \left({}_b\omega_1\right)_i {}^b\$^1{}_i + \left({}_1\omega_2\right)_i {}^1\$^2{}_i + \left({}_2\omega_t\right)_i {}^2\$^t{}_i. \quad (6) $$

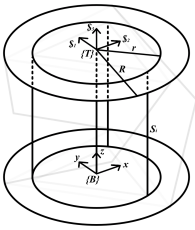

Figure 5. Plücker coordinates and reference frames.

IV. Conclusion

This paper reports a design that satisfies the requirements of a conventional single 3-DOF spatial mechanism without the use of motors for rotational motion. The 3RRR slanted arm inspired by the Kresling origami design achieves the rotational motion required for wrist prosthetics. This provides a basis for the many parallel mechanism-inspired wrist prosthetics that are unable to perform rotational pronating and supinating motions. The ability of the design to perform spherical movements also allows the proposed design to function with the requirements of a conventional 3-DOF spatial design.

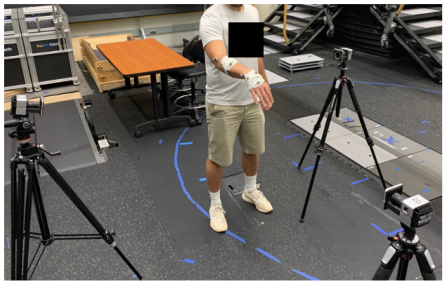

Figure 6. Motion capture set up.

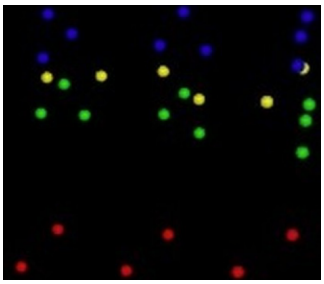

Figure 7. Motion capture 3D visualization that shows an arm pronating, at rest, and supinating.

Presented was a preliminary analysis before a physical prototype of the model was constructed. The model is expected to be 3D printed and manufactured to validate the results of the analysis. The proposed design also provides a basis for a novel prosthetic wrist for trans-radial amputees controlled through surface electromyography and actuated using motion capture data. Surface electromyography (sEMG) has already proven to be successful in allowing prosthetic rehabilitation patients to control limbs and joints with high precision using the remaining muscles and nerves from post-amputation stumps. [16] Further research is being conducted on training a regression model with surface electromyography and motion capture data. Surface electromyography data has been collected from forearm muscles present in trans-radial amputee stumps as shown in fig. 6 while motion capture data on the wrist has been obtained using the marker setup shown in fig. 7. Research is being conducted on the optimal regression method and feature sets to use. The regression model will be used to calculate the extent, speed, and direction of wrist motion and will be used to control the actuators of the proposed mechanism through sEMG signals.

V. Acknowledgment

We thank K. Herrin and B. Shafer from the Exoskeleton and Prothesis Intelligent Controls Lab for the motion capture data acquisition set-up and for the helpful discussions on the marker locations. We are also grateful to the CREATE-X team and the CREATE-X Idea2Prototype program for providing facilities, resources, and funding to aid our research.

References

[1] M. P. Fahrenkopf, N. S. Adams, J. P. Kelpin, V. H. Do. Hand Amputations. *Eplasty*. 2018;18:ic21. Published 2018 Sep 28.

[2] National Academies of Sciences, Engineering, and Medicine; Health and Medicine Division; Board on Health Care Services; Committee on the Use of Selected Assistive Products and Technologies in Eliminating or Reducing the Effects of Impairments; Flaubert JL, Spicer CM, Jette AM, editors. The Promise of Assistive Technology to Enhance Activity and Work Participation. Washington (DC): National Academies Press (US); 2017 May 9. 4, Upper-Extremity Prostheses. Available from: https://www.ncbi.nlm.nih.gov/books/NBK453290/

[3] B. D. Adams, N. M. Grosland, D. M. Murphy, and M. McCullough, paired wrist motion on hand and upper-extremity *J. Hand Surg. Am.*, vol. 28, no. 6, pp. 898903, Nov. 2003.

[4] N. A. Abd Razak, N. A. Abu Osman, M. Kamyab, W. A. Wan Abas, H. Gholizadeh, "Satisfaction and problems experienced with wrist movements: comparison between a common body-powered prosthesis and a new biomechatronics prosthesis." *Am J Phys Med Rehabil*. 2014;93(5):437-444. doi:10.1097/PHM.0b013e3182a51fc2

[5] Arthur Zinck, øyvind Stavdahl, Edmund Biden, and Peter J. Kyberd. "Design of a compact, reconfigurable, prosthetic wrist." *Appl. Biomechanics 9*, 2012, pp. 117-124

[6] N. M. Bajaj, A. J. Spiers and A. M. Dollar, "State of the art in prosthetic wrists: Commercial and research devices," *2015 IEEE International Conference on Rehabilitation Robotics (ICORR)*, 2015, pp. 331-338, doi: 10.1109/ICORR.2015.7281221.

[7] S. Valeria and P. Dmitry, "Design of the Parallel Spherical Manipulator for Wrist Rehabilitation," *2019 3rd School on Dynamics of Complex Networks and their Application in Intellectual Robotics (DCNAIR)*, 2019, pp. 166-168, doi: 10.1109/DCNAIR.2019.8875585.

[8] J. P. Merlet., C. Gosselin. "Parallel Mechanisms and Robots. In: Siciliano B., Khatib bO." *Springer Handbook of Robotics.* 2008; https://doi.org/10.1007/978-3-540-30301-5_13

[9] J. A. Leal-Naranjo., M. Wang., J. C. Paredes-Rojas., "Design and kinematic analysis of a new 3-DOF spherical parallel manipulator for a prosthetic wrist." *J Braz. Soc. Mech. Sci. Eng.* 2020, pp. 63, https://doi.ort/10.1007/s40430-019-2153-5

[10] S. Kumar., B. Bongardt., M. Simnofske., "Design and Kinematic Analysis of the Novel Almost Spherical Parallel Mechanism Active Anke." *J Intell Robot Syst*, 2019, pp. 303-325, https://doi.org/10.1007s/10846-018-0792-x

[11] T. S. Kim., D. D. Park., Y. B. Lee., D. G. Han., J. S. Shim., Y. J. Lee., P. C. Kim., "A study on the measurement of wrist motion range using the iPhone 4 gyroscope application," *Ann Plast Surg,* 2014, pp. 215-218, doi:10.1097/SAP.0b013e31826eabfe

[12] *Visual dictionary Online*. HUMAN BEING :: ANATOMY :: SKELETON :: TYPES OF SYNOVIAL JOINTS [2] image - Visual Dictionary Online. (n.d.). http://www.visualdictionaryonline.com/human-being/anatomy/skeleton/types-synovial-joints_2.php.

[13] N. Kidambi., K. W. Wang., "Dynamics of Kresling Origami Deployment," arXiv:10.1103/PhysRevE.101.063003

[14] Paul, R. P., 1981, *Robot Manipulators: Mathematics, Programming, and Control*, MIT Press, Cambridge, Massachusetts.

[15] C. D. Crane., J. M. Rico., J. Duffy., Screw Theory and Its Applications to Spatial Robot Manipulators, *Unpublished Work,* pp. 174-76

[16] L. Resnik., H. Huang, (., Winslow, A. *et al.* Evaluation of EMG pattern recognition for upper limb prosthesis control: a case study in comparison with direct myoelectric control. *J NeuroEngineering Rehabil* **15,** 23 (2018). https://doi.org/10.1186/s12984-018-0361-3